EASR

Engineering and Applied Science Research

https://www.tci-thaijo.org/index.php/easr/index

Published by the Faculty of Engineering, Khon Kaen University, Thailand

Optimization of oxygen transfer coefficient and standard aeration efficiency of a Venturi-type aerator using response surface methodology

Aphirak Khadwilard[1)], Manop Pipathattakul*[2)] and Prayoon Surin[1)]

[1)]Department of Advanced Manufacturing Technology, Faculty of Engineering, Pathumwan Institute of Technology, Bangkok 10330, Thailand
[2)]Department of Mechanical Engineering, Faculty of Engineering, Pathumwan Institute of Technology, Bangkok 10330, Thailand

Received 23 April 2025
Revised 9 November 2025
Accepted 18 November 2025

Abstract

This research focuses on determining the optimal parameters for maximizing dissolved oxygen (DO) when using a Venturi-type aerator, considering two objectives: oxygen transfer coefficient corrected to 20°C (K_La_{20}) and standard aeration efficiency (SAE). The determination of the optimal parameters for the Venturi-type aerator was carried out under thirty experimental conditions of a face-centered central composite design (FCCD), involving four influencing variables: Venturi convergence angle (α), Venturi divergence angle (β), water flow rate (Q_w), and air flow rate (Q_a). Response surface methodology (RSM) was used to evaluate the experimentally collected data. The analysis of the experimental results showed that the most suitable conditions for K_La_{20} were 45° convergence angles and 15° divergence angles, with a water flow rate of 40 L/min and an air flow rate of 0.9 L/min, resulting in a K_La_{20} value of 4.278 h^{-1}. For optimal SAE values, the study found that the Venturi convergence angle of 45°, the Venturi divergence angle of 15°, the water flow rate of 20 L/min, and the air flow rate of 0.9 L/min should be set. These parameters gave an SAE value of 0.0343 kgO_2/kWh. Analysis of the regression equations developed in this study showed that the coefficients of determination (R^2) of the K_La_{20} and SAE prediction equations were more than 90% for both equations. Therefore, the response can be accurately predicted, and these equations serve as guidelines for the design of the most appropriate Venturi-type aerator in practice.

Keywords: Venturi-type aerator, Response surface methodology, Standard aeration efficiency, Oxygen transfer coefficient

Nomenclature

C	Dissolved oxygen concentration (mg/L)	V	Volume of water in reservoir (m^3)
C_∞^*	Saturation dissolved oxygen concentration at steady state (mg/L)	P	Power input to aerator (kW)
C_0	Initial dissolved oxygen concentration (mg/L)	α	Convergence angle (°)
K_La	Volumetric oxygen transfer coefficient (h^{-1})	β	Divergence angle (°)
K_La_{20}	Volumetric oxygen transfer coefficient corrected to 20°C (h^{-1})	Q_w	Water flow rate (L/min)
SAE	Standard aeration efficiency (kgO_2/kWh)	Q_a	Air flow rate (L/min)
$SOTR$	Standard oxygen transfer rate (kgO_2/h)		

1. Introduction

Dissolved oxygen (DO) plays a crucial role in both wastewater management and aquaculture, influencing the functioning of aquatic organisms and the treatment process. Fish growth benefits from adequate dissolved oxygen concentrations for fish respiration, as low oxygen levels are harmful to fish. However, adequate oxygen levels support metabolic processes and improve food conversion for growth [1]. Wastewater treatment systems rely heavily on dissolved oxygen, as it is a key factor in the extraction of nutrients and pollutants from water. The biomass generated by aquaculture processes that consume wastewater creates added value for water purification, independent of other benefits [2]. Sufficiently elevated oxygen concentrations reduce organic matter in the effluent, resulting in improved water quality [2]. Conventional artificial aeration systems used for wastewater dissolved oxygen management are energy intensive and costly, as they are often operated continuously without precise control, resulting in excessive aeration relative to the actual oxygen demand of the system [3]. Approaches to dissolved oxygen management in aquaculture and wastewater treatment systems require careful consideration, balancing energy consumption with efficiency and cost-effectiveness outcomes.

Venturi-type aerators present several advantages over traditional aeration methods. They are efficient and cost-effective devices, and their simple design makes them ideal for wastewater treatment. Recently introduced design improvements have shown that Venturi-type aerators can achieve high efficiency, with oxygen transfer rates of up to 0.105 kgO_2/kWh [4]. A recent sludge reduction method has demonstrated a dissolution rate of 35.3%, which exceeds the 28.6% efficiency level of conventional disc aerators [5]. The simple construction of Venturi-type aerators, with no moving parts, makes them highly durable and less prone to failure during operation.

*Corresponding author.
Email address: manop@pit.ac.th
https://doi.org/10.64960/easr.2026.261795

They also require minimal maintenance, as there are no complex components or frequent calibrations, making them an ideal choice for wastewater treatment applications [6]. The basic structure of Venturi-type aerators results in a reliable and robust device, enabling long-term stable operation [7]. Additionally, since they are inexpensive and energy-efficient, the installation process for these devices is simpler than that of traditional compressor systems. This results in significant reductions in operating costs and infrastructure costs [8]. However, the performance of Venturi-type aerators under various conditions may not meet current aeration system standards. Therefore, further research is needed to enhance their applicability in a wide range of applications.

The geometric parameters of the Venturi-type aerator, including the confluence and divergence angles, directly affect the dynamics of bubble formation, which in turn affects the oxygen transfer level in the water body. Bubble formation within the depressurization zone of the Venturi tube depends on the convergence angle geometry, as a steeper convergence angle increases the liquid velocity, forming small bubbles with high air retention, thus improving the oxygen transfer efficiency for aquaculture [9, 10]. The size of the divergence angle determines how uniformly the bubbles grow and disperse, while also influencing the bubble burst diameter and performance. Different design parameters of the divergence angle significantly affect both the average bubble diameter and the aeration efficiency [11, 12]. The air-water mixing efficiency depends on the length-to-diameter ratio of the throat section, which, in particular, produces small air bubbles for improved aeration capacity [9, 13]. In addition to geometric parameters, the design of a Venturi-type aerator must also consider the water flow rate and air flow rate, as these factors will also affect the optimal performance of the aerator.

Engineering applications have adopted Response Surface Methodology (RSM) as a standard tool for aerator design. RSM is an efficient technique for optimizing studied variables to determine the aeration efficiency level. RSM is a statistical mathematical procedure that examines the relationship between independent factors and their responses. This tool shows suitable applications in environmental engineering as well as manufacturing applications. During aeration design, RSM uses a polynomial model to generate a response surface that identifies the optimal operating conditions that are beneficial for improving efficiency [14]. Furthermore, studies on the optimization of axial flow fans for aeration systems utilize impeller designs and assembly methods to achieve higher efficiency [15]. Studying the effects of different operating parameters on wastewater treatment efficiency through RSM has been proven to be effective in improving water quality for waste management while accelerating pollutant removal [16, 17]. In the aerator construction process, analyzing the effects of air flow rate due to compression is crucial, as neglecting this factor can result in a decrease in efficiency. Through RSM, the optimal design parameters, including the factors that affect compression, can be detected to optimize the efficiency when operating under different conditions [18]. RSM represents an efficient and systematic approach to optimizing the aeration process in complex engineering applications. In the case of Venturi-type aerators, RSM helps in understanding the optimal operating parameters such as convergence angle, divergence angle, water flow rate, and relative air flow rate based on mathematical models describing experimental data. This efficient approach reduces the number of tests, saves resources, and helps in finding the conditions that can provide the most efficient aeration performance. Therefore, this research aims to find the best configuration for using Venturi-type aerators to increase the dissolved oxygen content by considering the response of oxygen transfer coefficient corrected to 20 °C ($K_L a_{20}$) and standard aeration efficiency (SAE).

2. Materials and methods

2.1 Experimental apparatus and venturi-type aerator

As shown in Figure 1, the experimental apparatus was constructed as a Venturi-type aeration system. Water was circulated from the reservoir to the storage tank by a centrifugal pump (VENZ, VM 100, 1 HP, Q 20–100 L/min, H 33-35 m) controlled by an inverter. As water flowed through the Venturi-type aeration device, air was sucked into the throat to mix with water for aeration. Meanwhile, air was supplied by a diaphragm compressor (MEGA, 600, 3 W, Q 1–2 L/min) with a typical discharge pressure of approximately 18 kPa and was controlled by a needle valve to maintain constant flow conditions**.**

In the experimental process, measuring instruments were used to monitor the operating parameters during the experiment. The water flow rate was measured with a rotameter (SHUNHUAN, LZM-40G, range: 10–70 L/min, ±4% F.S.), while the air flow rate was measured with a rotameter (NOVFDLOP, LZT-6T, range: 0.1–1 L/min, ±4% F.S.). The dissolved oxygen concentration in the water tank was continuously measured using a DO probe connected to a DO meter (Lutron DO-5519, range: 0-20 mg/L, accuracy ±0.4 mg/L), which were the necessary data for evaluating the aeration efficiency.

Figure 2 shows a cross-sectional view of the Venturi aerator used in this research to create a pressure differential for mixing or suctioning liquids. The aerator has an inlet and outlet diameter of 25 mm, a throat diameter of 12.5 mm, and a 3 mm air orifice at the throat. As water flows through the throat, the water velocity increases, thus decreasing the pressure at the throat, allowing aeration. After the inlet and before the outlet, there are convergence (α) and divergence (β) angles that control the flow characteristics, which in turn affect the aeration efficiency.

In this study, the diameter of the Venturi throat was set to 12.5 mm. The size of the Venturi throat diameter is an important parameter influencing the bubble generation and aeration efficiency [9,13], however, varying the size of the Venturi throat diameter was beyond the scope of this study. This decision was made to isolate the effects of the convergence and divergence angles as well as the water and air flow rates, which were the main variables of interest.

The experimental design considered a series of convergence and divergence angles of 15°, 30°, and 45°, as recommended in the literature. Lee et al. [19] systematically studied the outlet angles in this range and proved that a 30° outlet angle provides optimum conditions for microbubble formation, depressurization, and air suction, while angles greater than 45° cannot effectively maintain microbubble formation. Similarly, Sakamatapan et al. [20] also used 30° angles for convergence and divergence angles, emphasizing the appropriate design fit to maximize air intake. Therefore, the use of these angles not only supports microbubble formation but also correlates with the oxygen transfer coefficient ($K_L a$) and standard aeration efficiency (SAE). Consequently, convergence and divergence angles of 15°, 30°, and 45° were selected in this research. These angles allow for systematic investigation of the relationship between Venturi-type aerator geometry and optimal aeration efficiency.

Although the water flow rate was controlled by adjusting the pump motor speed via an inverter, flow rate variations invariably affected the inlet pressure. This is because both inlet pressure and throat pressure are important factors in the rupture of air bubbles and the solubility of oxygen. In this study, system pressure was not initially considered, but it was measured during the experiment using a pressure gauge (WIKA, pgs63). The results of the pressure measurements when the water flow rate was varied, ranging from 3-13 kPa, which is a relatively low pressure. Therefore, the lack of consideration of water pressure represents a limitation of this experiment. Meanwhile, the air flow rate was measured by volume rather than by actual mass. Although this practice is commonly accepted in the

literature for laboratory aeration experiments conducted near ambient conditions, the effect of compression is neglected. Therefore, the reported values should be interpreted as approximate volumetric flow rates under laboratory conditions.

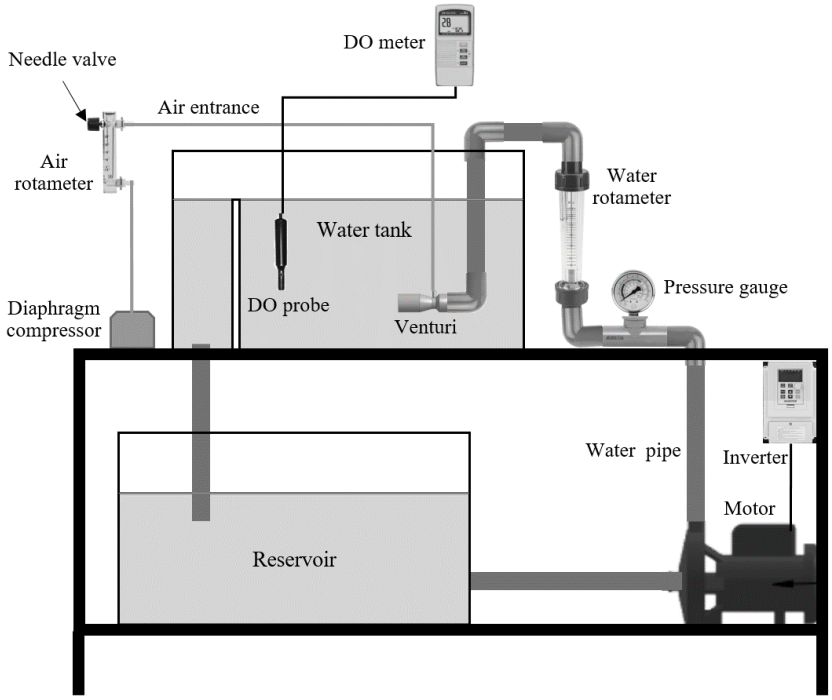

Figure 1 Schematic of the experimental apparatus.

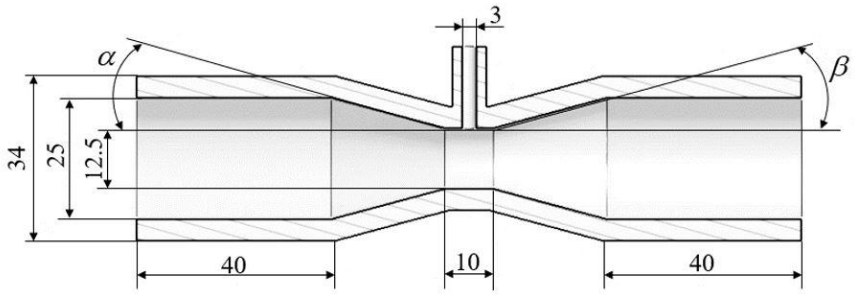

Figure 2 Model of the Venturi-type aerator.

In this study, volumetric flow rates (L/min) were measured using a rotameter, without direct measurement of mass flow rates. For air, as it is a compressible fluid, sudden pressure drops at the control valve can change both density and temperature, which may affect oxygen solubility and transfer dynamics. Although these effects are expected to be minimal under the relatively low-flow conditions studied, they represent a limitation of this research.

In compliance with ASCE clean water standards [21], the experiments were carried out in clean tap water at 25 ± 1°C. A reservoir volume of 90 L was maintained for each trial. Water was taken at 25°C to have a density of 997 kg/m^3 and a dynamic viscosity of 0.890×10^{-3} Pa·s. Aeration air was taken to have standard properties at 25°C and 1 atm, i.e., a density value of 1.184 kg/m^3 and a viscosity of 1.849×10^{-5} Pa·s. No salts or other impurities were added except those necessary for the deoxygenation chemicals.

This study was conducted using an experimental setup, as shown in Figure 1. In the initial stage of the aeration test, the water was deoxygenated with 8-10 ppm sodium sulfite and 0.05-0.1 ppm cobalt chloride per 1 ppm dissolved oxygen uptake, respectively [21, 22]. The mixer was operated until the DO was reduced to near 0 mg/L. Equation (1) shows the mechanism of DO concentration reduction by sodium sulfite with cobalt chloride acting as a catalyst:

$$Na_2SO_3 + \frac{1}{2}O_2 \rightarrow Na_2SO_4 \quad (1)$$

2.2 Theoretical analysis of aeration

Evaluating oxygen transfer in clean water [21] requires performing a defined oxygen transfer test, which allows researchers to measure the oxygen transfer rate expressed as the mass of dissolved oxygen per unit volume of time. This measurement method works equally well with standard activated sludge wastewater treatment processes and small laboratory oxygenation devices. It is used efficiently under a variety of operating conditions. The standardized oxygen transfer rate (SOTR) is the primary outcome of this test, as it provides an assessment of the theoretical oxygen mass transfer under specific conditions, including zero dissolved oxygen at 20°C

and 1 atm pressure. The method is primarily designed for the analysis of pure water. The oxygen transfer rate in process water can be calculated by using experimental data for the evaluation.

2.2.1 Oxygen transfer coefficient (K_La)

The standard oxygen transfer model appears as a mass balance equation that tracks the change in dissolved oxygen (DO) concentration in water with respect to time as shown in equation (2) [19].

$$\frac{dC}{dt} = K_L a(C_\infty^* - C_0) \tag{2}$$

Equation (2) is integrated to provide the expression as a function of time, given in Equation (3), assuming that DO saturation concentration remains constant throughout the testing period.

$$C = C_\infty^* - (C_\infty^* - C_0)\exp(-K_L a \times t) \tag{3}$$

where C (mg/L) is the DO concentration, C_∞^* (mg/L) is the steady-state DO saturation concentration at the determination point as time approaches infinity, C_0 (mg/L) is the DO concentration at time zero, and K_La (h^{-1}) is the apparent volumetric mass transfer coefficient at the determination point.

The ASCE advises data analysis through nonlinear regression using the Gauss-Newton method, which fits Equation (3) with parameters K_La, C_0, and C_∞^* as adjustable variables. The statistical values of K_La get adjusted to standard conditions of 1 atm pressure and 20°C water temperature through the calculation shown below as Equation (4).

$$K_L a_{20} = K_L a\,\theta^{(20-T)} \tag{4}$$

where K_La_{20} (h^{-1}) is the determination point value of K_La corrected temperature to 20°C, and a generally accepted value of the temperature correction factor, θ, is 1.024 for clean water [21].

2.2.2 Standard oxygen transfer rate

The standard oxygen transfer rate (SOTR) is one of the most important parameters that can be used to assess the performance of aeration systems under standard conditions, especially for clean water. The SOTR of clean water, defined as the mass of oxygen transferred from ambient air into water per unit time under standard conditions, is usually expressed in kilograms of oxygen per hour (kgO_2/h). It is an important parameter in designing and evaluating the performance of aeration systems used in wastewater treatment. The main equation for calculating SOTR is shown in Equation (5).

$$SOTR = K_L a_{20} \times C_{\infty 20}^* \times V \tag{5}$$

where $C_{\infty 20}^*$ (mg/L) is the determination point value of the steady-state DO saturation concentration as time approaches infinity at 20°C and V (m^3) is the tank's water volume.

2.2.3 Standard aeration efficiency

Equation (6) can be used to determine the Standard Aeration Efficiency (SAE), which is important in selecting an aerator for applications, as it relates to the oxygen transfer rate per unit of electrical power used.

$$SAE = \frac{SOTR}{P} \tag{6}$$

where P represents the power input to the aerator, measured in kilowatts (kW).

In this study, the electrical power input (P) to the aerator used in SAE calculation was defined as the sum of the electrical power consumed by the circulating pump motor and the diaphragm compressor. The power consumption of each device was measured using a digital power meter and reported in kilowatts (kW).

2.3 Experimental design for response surface methodology

The experimental design for increasing dissolved oxygen using a Venturi-type aerator was performed using a face-centered central composite design (FCCD). The FCCD used in this study consisted of factorial points, axis points positioned at the center of each face of the designed cube, and multiple replicates at the center point. This approach allows for robust quadratic models. Response Surface Methodology (RSM) then uses these FCCD data sets to estimate second-order polynomial regression coefficients (Eq. 7), thus describing the response surfaces of K_La_{20} and SAE as functions of the four control parameters. The independent factors (Table 1) were the inlet angle (15°- 45°), outlet angle (15°- 45°), water flow rate (20 L/min - 40 L/min), and air flow rate (0.1 L/min - 0.9 L/min). Two dependent variables were measured to represent the oxygen transfer coefficient at 20 °C (K_La_{20}) and the standard aeration efficiency (SAE) of the Venturi-type aerator. The RSM experimental design was created by Minitab software to develop a quadratic model that fit the experimental data, to plot the three-dimensional response surfaces, and to optimize the parameters of the Venturi-type aerator.

In this study, three levels of independent variables were set, and 30 conditions were tested to predict the optimization process. The estimation of pure error sums of squares was repeated six times at the center of the experiment, and the interactions between the independent variables and their responses are shown in Table 2. The quadratic models and regression equations are derived from the

experimental values. Generally, we take a specific set of independent variables and apply a low-degree polynomial to model the response. The first-order model serves as the estimator function when the response is well described by a linear function of the independent variables. In cases where the system exhibits curvilinear behavior, a higher-degree polynomial model, such as a second-order model, is required. As shown in Equation (7), a quadratic regression model is used.

Table 1 Independent factors and its range set in experiment design.

Input variables	Unit	Levels		
		-1	0	1
A: Convergence angle	-º	15	30	45
B: Divergence angle	-º	15	30	45
C: Water flow rate	L/min	20	30	40
D: Air flow rate	L/min	0.1	0.5	0.9

$$Y = \beta_0 + \sum_{i=1}^{n} \beta_i X_i + \sum_{i=1}^{n} \beta_{ii} X_i^2 + \sum_{i<j}^{n} \beta_{ij} X_i X_j + \varepsilon \quad (7)$$

where Y represents the response value, such as $K_L a_{20}$ (h^{-1}), SAE (kgO_2/kWh), and β_0 is a constant. In addition, X_i and X_j represent the input independent variables, with n being the number of free parameters involved in the experiment. The coefficients of the regression model, linear equations, quadratic equations, and interaction equations, are denoted by β_i, β_{ii}, and β_{ij}, respectively. The response effects of the variables can be displayed as a three-dimensional surface graph by holding other variables constant, and the significance of the P value, R^2, and adjusted R^2 values were evaluated, where the R^2 value should be greater than 90% for the best fit of the regression model.

Table 2 Optimization of Venturi-type aerator parameters for $K_L a_{20}$ and SAE using RSM.

Run	Factors				$K_L a_{20}$ (h^{-1})		SAE (kgO_2/kWh)	
	A (º)	B (º)	C (L/min)	D (L/min)	Experiment	Prediction	Experiment	Prediction
1	15	15	20	0.1	1.9964	2.1889	0.023774	0.024599
2	45	15	20	0.1	2.7440	2.7868	0.030092	0.029663
3	15	45	20	0.1	1.9542	1.7726	0.021990	0.018820
4	45	45	20	0.1	1.9621	1.8935	0.021065	0.020464
5	15	15	40	0.1	3.3292	3.1381	0.019808	0.016703
6	45	15	40	0.1	4.1380	4.0600	0.021841	0.021767
7	15	45	40	0.1	2.8149	2.9738	0.014154	0.014524
8	45	45	40	0.1	3.4171	3.4187	0.017795	0.016168
9	15	15	20	0.9	2.5401	2.3759	0.029024	0.028826
10	45	15	20	0.9	3.1776	2.9738	0.036666	0.033890
11	15	45	20	0.9	2.2278	2.2165	0.025419	0.024906
12	45	45	20	0.9	2.2500	2.3374	0.026146	0.026550
13	15	15	40	0.9	3.2522	3.3251	0.016125	0.015362
14	45	15	40	0.9	4.0890	4.2470	0.019247	0.020426
15	15	45	40	0.9	3.5302	3.4177	0.017160	0.015042
16	45	45	40	0.9	4.0199	3.8626	0.019266	0.016686
17	15	30	30	0.5	2.4843	2.5791	0.018629	0.019848
18	45	30	30	0.5	3.1273	3.1005	0.025132	0.023202
19	30	15	30	0.5	3.0968	3.1192	0.023393	0.024849
20	30	45	30	0.5	2.6729	2.7189	0.020767	0.020090
21	30	30	20	0.5	2.2343	2.4096	0.025387	0.026910
22	30	30	40	0.5	3.7558	3.6468	0.019073	0.018030
23	30	30	30	0.1	3.1433	3.0765	0.022206	0.021283
24	30	30	30	0.9	3.2570	3.3920	0.025498	0.023656
25	30	30	30	0.5	3.1294	3.0282	0.024107	0.022470
26	30	30	30	0.5	3.1831	3.0282	0.024968	0.022470
27	30	30	30	0.5	3.0599	3.0282	0.023396	0.022470
28	30	30	30	0.5	3.2569	3.0282	0.025046	0.022470
29	30	30	30	0.5	3.0112	3.0282	0.023125	0.022470
30	30	30	30	0.5	2.9870	3.0282	0.023141	0.022470

3. Results and discussion

3.1 Experimental results for $K_L a_{20}$ using response surface methodology

The oxygen transfer coefficient ($K_L a$) was determined from aeration experiments, as shown in Figure 3. Dissolved oxygen (DO) concentration increased exponentially toward saturation (Figure 3(a)), while the DO deficit (C_∞^* - C_t) decayed exponentially with excellent agreement between the experimental data and the model (R^2 = 0.9826, Figure 3(b)). From the slope of the fitted line, $K_L a$ was calculated as 0.08 min^{-1}, reflecting the aeration efficiency. This parameter is critical because it provides the foundation for standardizing oxygen transfer performance: $K_L a$ values measured experimentally can be normalized to 20°C ($K_L a_{20}$) for system-to-system comparison and subsequently used to calculate the standard aeration efficiency (SAE), a key indicator for assessing and

comparing aerator performance under varying conditions. The presented value is provided here as an illustrative case, obtained under test conditions with a Venturi convergence angle of 45°, a Venturi divergence angle of 15°, a water flow rate of 20 L/min, and an air flow rate of 0.9 L/min.

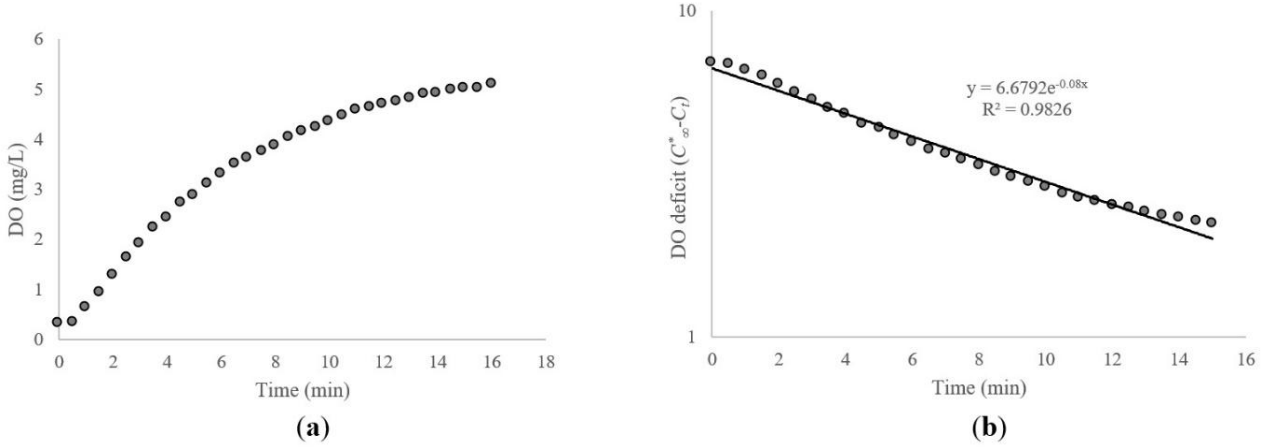

Figure 3 Aeration curves. (a) Increase in dissolved oxygen; (b) Dissolved oxygen deficit.

Analysis of Variance (ANOVA) was employed to evaluate the significance of each factor and interaction in the quadratic response surface models. ANOVA tests whether the variation explained by the model is statistically greater than the residual error. The statistical model has been validated using ANOVA for the quadratic response surface methodology. The ANOVA results for $K_L a_{20}$ provide evidence of a robust, significant ($P < 0.01$) model that describes the variation in the response variable adequately, as shown in Table 3. Water flow rate ranked highest among factors that influenced the dependent variable, with the highest F-value of 288.24. All main factors, convergence angle, divergence angle, water flow rate, and air flow rate, show significant effects ($P < 0.01$). Some two-level interactions are also highly significant, especially those involving the convergence angle. The quadratic terms show a marginal significance ($P = 0.056$), which suggests that they might contribute some slight non-linearity. More importantly, it should be noted that the lack of fit is not significant ($P = 0.138$), indicating that the model indeed fits the data well. This suggests that $K_L a_{20}$ is determined by a complex system encompassing linear effects, interactions, and possible nonlinear relations.

Table 3 ANOVA estimated for $K_L a_{20}$

Source	DF	Adj SS	Adj MS	F-Value	P-Value
Model	11	10.1505	0.92277	37.76	0.000
Linear	4	9.4571	2.36428	96.75	0.000
A: Convergence angle	1	1.2777	1.27771	52.29	0.000
B: Divergence angle	1	0.6861	0.68612	28.08	0.000
C: Water flow rate	1	7.0437	7.04366	288.24	0.000
D: Air flow rate	1	0.4496	0.44962	18.40	0.000
Square	3	0.2229	0.07431	3.04	0.056
Convergence angle*Convergence angle	1	0.1006	0.10057	4.12	0.058
Divergence angle*Divergence angle	1	0.0338	0.03381	1.38	0.255
Air flow rate*Air flow rate	1	0.1206	0.12062	4.94	0.039
2-Way Interaction	4	0.4704	0.11760	4.81	0.008
Convergence angle*Divergence angle	1	0.2277	0.22769	9.32	0.007
Convergence angle*Water flow rate	1	0.1093	0.10929	4.47	0.049
Divergence angle*Water flow rate	1	0.0673	0.06734	2.76	0.114
Divergence angle*Air flow rate	1	0.0661	0.06610	2.70	0.117
Error	18	0.4399	0.02444		
Lack-of-Fit	13	0.3853	0.02964	2.72	0.138
Pure Error	5	0.0545	0.01090		
Total	29	10.5903			
R-sq = 95.85%, R-sq(adj) = 93.31%, R-sq(pred)= 85.19					

The $K_L a_{20}$ model was constructed from 30 experimental data sets. The results of ANOVA analysis showed that $K_L a_{20}$ values were related to four factors, namely, convergence angle, divergence angle, water flow rate and air flow rate as determined by P values (Table 3). Since the second-order polynomial was statistically significant, a quadratic regression model was chosen for the response of $K_L a_{20}$ as shown in Equation (8).

$$K_L a_{20} = 0.534 + 0.0673\,A + 0.0137\,B + 0.000551\,C - 1.215\,D - 0.000837\,A^2 - 0.000485\,B^2 + 1.288\,D^2 - 0.000530\,A*B + 0.000009\,A*C + 0.000007\,B*C + 0.01071\,B*D \quad (8)$$

The quadratic regression model (Equation (8)) indicated that the model fitted the data well, with a coefficient of determination (R^2) of 95.85% and an adjusted coefficient of determination of 93.31%, respectively, confirming that the model had high accuracy in predicting the response.

The relationship between the oxygen transfer coefficient (K_La_{20}) and geometric and flow parameters can be determined from the 3D surface plots in Figure 4. The data in Figure 4(a) show how K_La_{20} increases as the divergence and convergence angles change. The data from the plots reveal that large inlet angles and small outlet angles result in increased K_La_{20}, indicating that geometric design is a key factor in optimizing oxygen transfer efficiency. The data in Figure 4(b) show that higher water flow rates lead to improved K_La_{20} due to increased turbulence. The data from Figure 4(c) reveal that K_La_{20} significantly increases in situations where both air and water flow rates increase simultaneously, as their interaction determines the mass transfer efficiency. A multivariate analysis shows that no single parameter acts independently to influence the efficiency, as they mutually affect the operational outcome. This evaluation proves that successfully optimizing the mass transfer efficiency of a fluid system depends on both flow velocity management and the geometric design of the Venturi to achieve optimal performance.

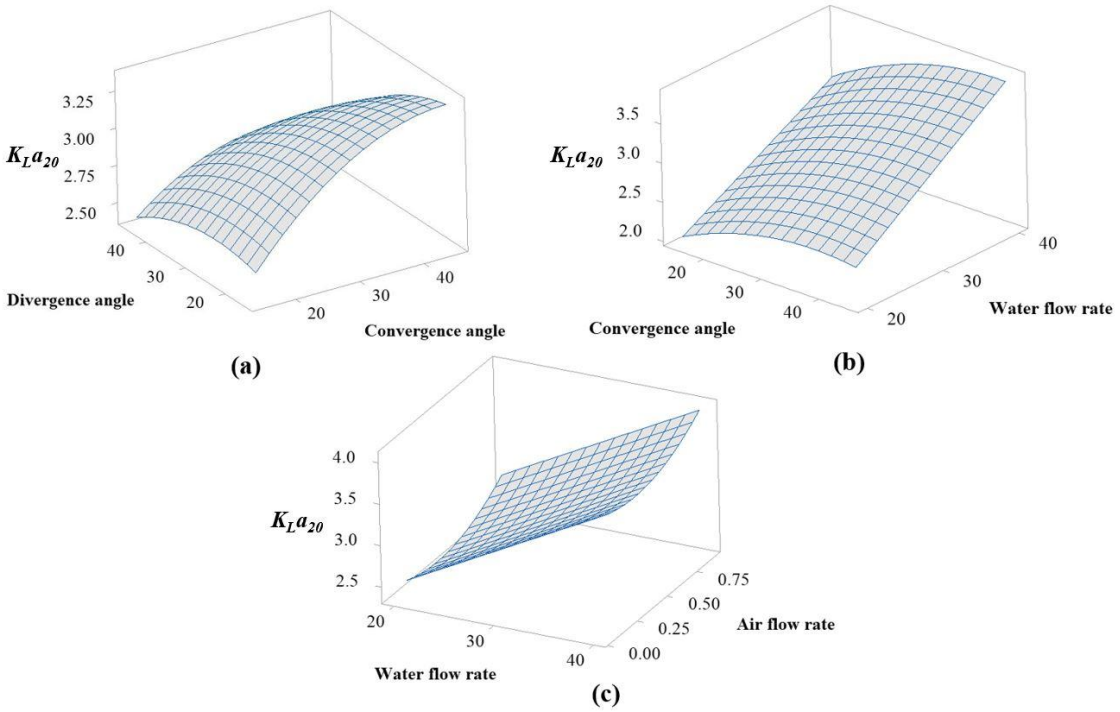

Figure 4 Three-dimensional plot for K_La_{20}

Considering the influence of the studied factors on the response, the analysis was undertaken to determine the optimal set of factors. The optimization analysis in Figure 5 specified the K_La_{20} value, where the desirability (D) value was 1.000, giving the maximum K_La_{20} value of 4.2788 h^{-1} under the existing constraints. The analysis examined the convergence angle, divergence angle, water flow rate, and air flow rate over a range of values. The analysis results showed that the convergence angle of 45°, the divergence angle of 17.12°, which are close to the lower end of the range (15°), the water flow rate of 40 L/min, and the air flow rate of 0.9 L/min, demonstrated the best oxygen transfer potential. It can be seen that the parameters of the Venturi-type aeration system affect the oxygen transfer capacity.

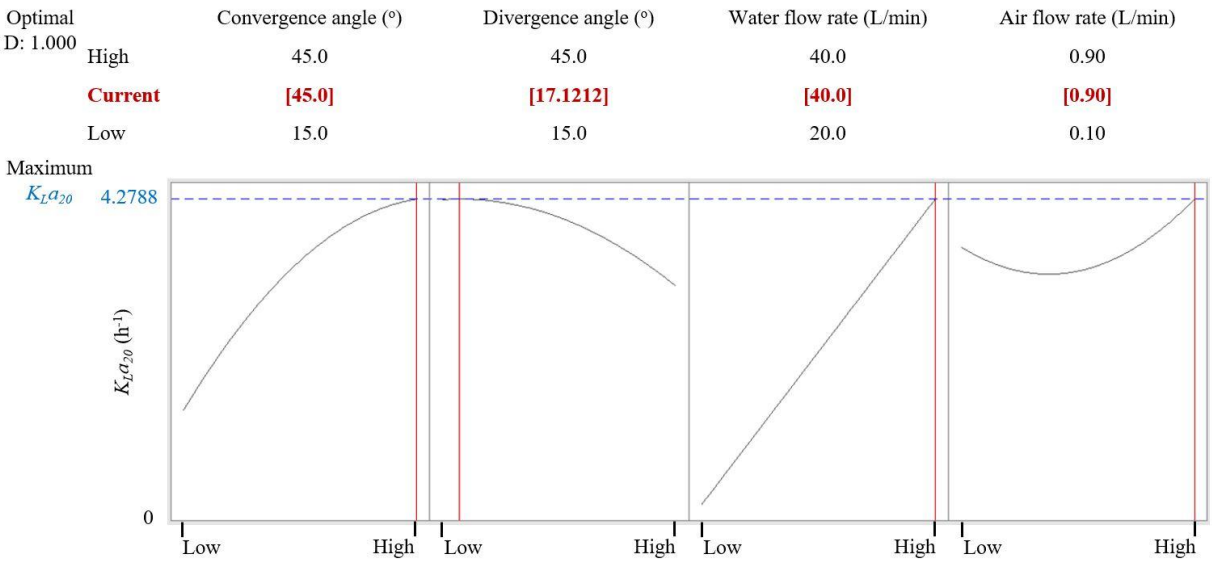

Figure 5 Optimal condition for maximum K_La_{20}

3.2 Experimental results for SAE using response surface methodology

The statistical model was validated using ANOVA for quadratic response surface method. The ANOVA results for SAE showed a reliable and significant model fit ($P < 0.01$), adequately explaining the variance of the response variable. As shown in Table 4, water flow rate had the greatest effect among the factors influencing SAE, with the highest F value of 123.95. All main factors, including convergence angle, divergence angle, water flow rate, and air flow rate all had significant effects ($P < 0.01$). The most significant pairwise interaction occurred when water flow rate was paired with air flow rate, while the quadratic term was not statistically significant. More importantly, it should be noted that the lack of fit was not significant ($P = 0.067$), indicating that the model fit the data well.

Table 4 ANOVA estimated for SAE

Source	DF	Adj SS	Adj MS	F-Value	P-Value
Model	9	0.000535	0.000059	23.52	0.000
Linear	4	0.000467	0.000117	46.15	0.000
A: Convergence angle	1	0.000054	0.000054	21.35	0.000
B: Divergence angle	1	0.000073	0.000073	28.82	0.000
C: Water flow rate	1	0.000313	0.000313	123.95	0.000
D: Air flow rate	1	0.000026	0.000026	10.47	0.004
Square	1	0.000006	0.000006	2.49	0.130
Convergence angle*Convergence angle	1	0.000006	0.000006	2.49	0.130
2-Way Interaction	4	0.000062	0.000016	6.15	0.002
Convergence angle*Divergence angle	1	0.000012	0.000012	4.55	0.045
Divergence angle*Water flow rate	1	0.000017	0.000017	6.56	0.019
Divergence angle*Air flow rate	1	0.000003	0.000003	1.37	0.256
Water flow rate*Air flow rate	1	0.000031	0.000031	12.11	0.002
Error	20	0.000051	0.000003		
Lack-of-Fit	15	0.000047	0.000003	3.98	0.067
Pure Error	5	0.000004	0.000001		
Total	29	0.000586			
R-sq = 91.37%, R-sq(adj) = 87.48%, R-sq(pred)= 72.77%					

The SAE model was constructed from 30 experimental data points. The results of ANOVA analysis showed that the SAE value was related to four factors, namely, convergence angle, divergence angle, water flow rate, and air flow rate, as determined by the P-value (Table 4). Since the second-order polynomial was statistically significant, a quadratic regression model was chosen for the SAE response as shown in Equation (9).

$$SAE = 0.02985 + 0.000478\,A - 0.000263\,B - 0.000007\,C + 0.01108\,D - 0.000004\,A^2 - 0.000004\,A*B + 0.0000001\,B*C + 0.000078\,B*D - 0.000006\,C*D \quad (9)$$

The quadratic regression model (Equation (9)) indicated that the model fitted the data well, with a coefficient of determination (R^2) of 91.37% and an adjusted coefficient of determination of 87.48%, respectively, confirming that the model had high accuracy in predicting the response.

Figure 6 shows three 3D surface plots illustrating the relationship between SAE response and process parameters, namely divergence angle, convergence angle, air flow rate, and water flow rate. The increase in SAE occurs with increasing convergence angle and decreasing divergence angle, as shown in Figure 6(a). The aeration efficiency improves significantly with increasing air flow rate, as shown in Figure 6(b). This is because improved oxygen supply improves process efficiency. The data in Figure 6(c) shows that SAE increases with increasing air flow rate; conversely, if the water flow rate increases, SAE decreases. This is because increasing water flow rate results in increasing energy consumption. It can be seen that adjusting the water flow rate plays a crucial role in making the aeration process efficient without excessive energy consumption.

Figure 7 shows the results of the optimization of SAE using the desirability function approach in RSM. The panels illustrate the effects of each factor on SAE when the rest of the factors remain at their optimum levels. The data on SAE (kgO_2/kWh) are shown on the vertical axis, and the ranges of the factors within which they were tested are shown on the horizontal axis. The High and Low marks indicate the limits of the experiment, and the Current value (marked in red) indicates the location where each factor performed optimally. The blue dotted line shows the estimated maximum SAE (0.0343 kgO_2/kWh), which was achieved with a convergence angle of 45°, a divergence angle of 15°, a water flow rate of 20 L/min, and an air flow rate of 0.9 L/min. The desirability score ($D = 0.8958$) being close to 1 indicates that the conditions are nearly optimal. The graphical pattern shows that the SAE value increases with increasing convergence angle and air flow rate, but decreases with increasing divergence angle and water flow rate. Optimal aeration results depend on the correct balance between geometric components and flow characteristics, since SAE relies on the Venturi geometry, high air flow rate, and an optimum water flow rate.

To provide a broader context for the present findings, the aeration performance obtained in this study was compared with results from existing literature and commercially available Venturi-type aerators. The comparison focused on key parameters including structural dimensions, oxygen transfer coefficient (K_La_{20}), and standard aeration efficiency (SAE). Table 5 summarizes these results.

As shown in Table 5, the K_La_{20} measured in this study (4.28 h^{-1}) is comparable to the range reported for small-scale Venturi-type aerators (3.5–4.5 h^{-1}) by Mobasher and Mahmoud [8], and consistent with the field performance values (2.5–5.0 h^{-1}) reported by Therrien et al. [6]. The SAE obtained in this work (0.0343 kgO_2/kWh) aligns closely with values reported in previous studies [6-8], although it is lower than the maximum efficiency of 0.105 kgO_2/kWh reported by Yadav et al. [4]. These findings indicate that the current system achieves performance comparable to practical Venturi-type devices, while also highlighting opportunities for further

improvement. In particular, optimization of throat geometry, convergence/divergence angles, and operating conditions may further enhance oxygen transfer efficiency.

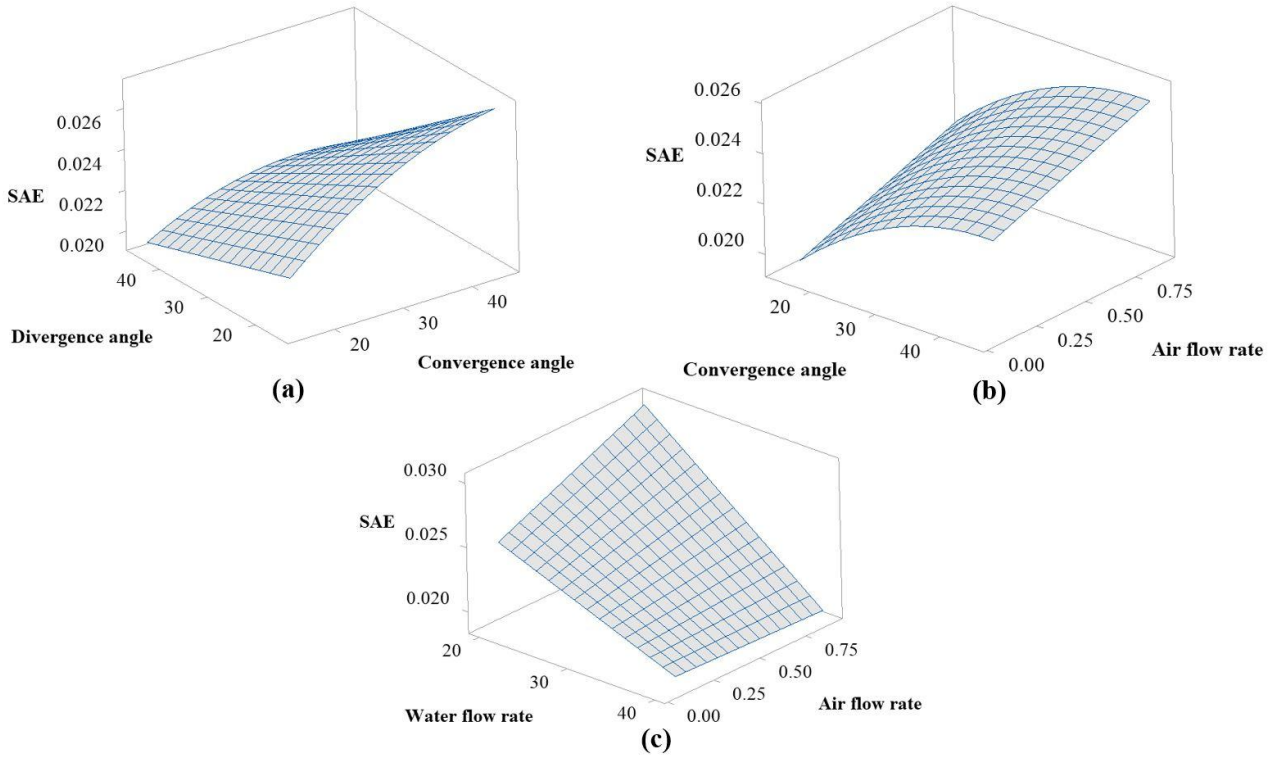

Figure 6 Three-dimensional plot for SAE

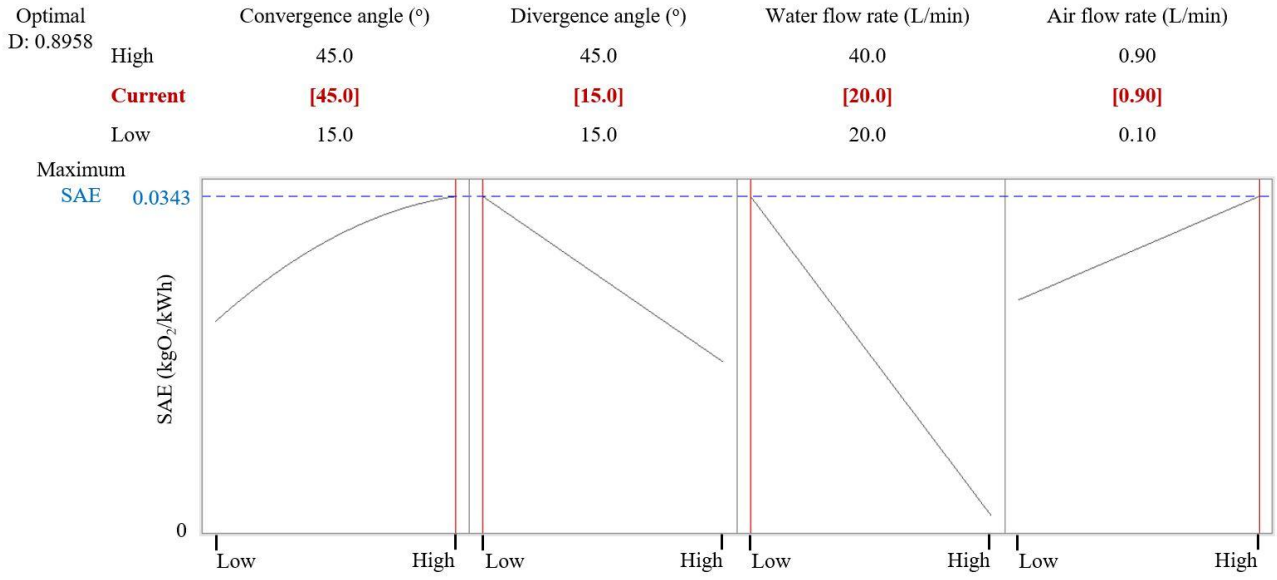

Figure 7 Optimal condition for maximum SAE.

Table 5 Comparison of Venturi-type aerator performance with existing literature and devices.

Study/Device	Convergence angle (°)	Divergence angle (°)	Throat diameter (mm)	$K_L a_{20}$ (h^{-1})	SAE (kgO_2/kWh)
This study	45	15	12.5	4.28	0.0343
Yadav et al. [4]	Not specified	Not specified	–	–	0.105
Li et al. [5]	CFD-optimized	CFD-optimized	–	–	0.035–0.050*
Therrien et al. [6]	Various	Various	–	2.5–5.0	0.020–0.040
Huang et al. [7]	Review	Review	–	–	0.025–0.045
Mobasher and Mahmoud [8]	20–45	15–30	~10–15	3.5–4.5	0.030–0.050

* approximate range based on reported efficiency improvements.

4. Conclusions

This research aimed to find the most suitable model for using a Venturi-type aerator to increase dissolved oxygen content in water by considering the oxygen transfer coefficient corrected to 20°C (K_La_{20}) and standard aeration efficiency (SAE). This objective was investigated through a face-centered central composite design**,** and the experimental results were analyzed by response surface methodology**.** In this study, four variables related to the increase in dissolved oxygen content were studied, namely, the Venturi convergence angle, the Venturi divergence angle, the water flow rate, and the air flow rate. A total of 30 experiments were conducted. The results showed that the most suitable conditions for the highest K_La_{20} value were 45° Venturi convergence angle, 15° Venturi divergence angle, 40 L/min water flow rate, and 0.9 L/min air flow rate. These parameters yielded a K_La_{20} value of 4.28 h^{-1}, with the R^2 of the mathematical model equal to 95.85%. Considering the best SAE value, the Venturi convergence angle of 45°, Venturi divergence angle of 15°, water flow rate of 20 L/min, and air flow rate of 0.9 L/min were found to be the most suitable. These parameters resulted in an SAE value of 0.0343 kgO_2/kWh, with the R^2 of the mathematical model equal to 91.37%. Therefore, the experimental regression equation could adequately describe the relationship among the four factors and could be used to accurately predict the K_La_{20} and SAE values for dissolved oxygen enhancement using a Venturi-type aerator. This research has the following limitations: The pressure and mass flow rate of the aeration system, as well as the geometry of the throat, which may affect the evaluation of oxygen transfer efficiency, were not considered. Therefore, future research should incorporate these variables to provide a more comprehensive evaluation of oxygen transfer efficiency, which may improve the efficiency and application of aerators.

5. References

[1] Li D, Zou M, Jiang L. Dissolved oxygen control strategies for water treatment: a review. Water Sci Technol. 2022;86(6):1444-66.
[2] Abinandan S, Subashchandrabose SR, Venkateswarlu K, Megharaj M. Nutrient removal and biomass production: advances in microalgal biotechnology for wastewater treatment. Crit Rev Biotechnol. 2018;38(8):1244-60.
[3] Valdez-Prudencio KM, Arceo-Diaz S, Bricio-Barrios JA, Bricio-Barrios EE. Mathematical model and experimental validation for the prediction of dissolved oxygen saturation in aquaculture ponds. J Phys Conf Ser. 2022;2153:012017.
[4] Yadav A, Roy SM, Biswas A, Swain B, Majumder S. Modelling and prediction of aeration efficiency of the venturi aeration system using ANN-PSO and ANN-GA. Front Water. 2024;6:1401689.
[5] Li H, Zhang Q, Zeng M, Cao J, Zhao Q, Hao L. Insights into gas flow behavior in venturi aerator by CFD-PBM model and verification of its efficiency in sludge reduction through O_3 aeration. J Water Process Eng. 2023;54:103960.
[6] Therrien JD, Vanrolleghem PA, Dorea CC. Characterization of the performance of venturi-based aeration devices for use in wastewater treatment in low-resource settings. Water SA. 2019;45(2):251-8.
[7] Huang J, Sun L, Liu H, Mo Z, Tang J, Xie G, et al. A review on bubble generation and transportation in venturi-type bubble generators. Exp Comput Multiphase Flow. 2020;2(3):123-34.
[8] Mobasher AM, Mahmoud AH. Effect of geometric characteristics on the aeration efficiency in the venturi system. J Al-Azhar Univ Eng Sect. 2021;16(60):650-65.
[9] Wilson DA, Pun K, Ganesan PB, Hamad F. Geometrical optimization of a venturi-type microbubble generator using CFD simulation and experimental measurements. Designs. 2021;5(1):4.
[10] Thoharudin T, Sunardi S, Yudha FAK, Nadjib M, Nugroho AS. Design and analysis of venturi microbubble generator using computational fluid dynamics. Eksergi. 2023;19(2):49-54.
[11] Basso A, Hamad FA, Ganesan P. Effects of the geometrical configuration of air–water mixer on the size and distribution of microbubbles in aeration systems. Asia Pac J Chem Eng. 2018;13(6):e2259.
[12] Noor S, Kaneko A. The breakup characteristics of bubbles in venturi tubes under different levels of dissolved gas. Jpn J Multiphase Flow. 2022;36(3):344-52.
[13] Ghannadi M, Saghravani SF, Niazmand H. Numerical analysis of water and air in venturi tube to produce micro-bubbles. J Rehabil Civ Eng. 2020;8:114-25.
[14] Bezerra MA, Santelli RE, Oliveira EP, Villar LS, Escaleira LA. Response surface methodology (RSM) as a tool for optimization in analytical chemistry. Talanta. 2008;76(5):965-77.
[15] Joseph CC, Anthony W, Anthony W. Response surface methodology in application of optimal manufacturing process of axial-flow fans adopted by modern industries. Am J Theor Appl Statist. 2018;7(6):235-41.
[16] Bashir MJK, Amr SA, Aziz SQ, Aun NC, Sethupathi S. Wastewater treatment processes optimization using response surface methodology (RSM) compared with conventional methods: review and comparative study. Middle East J Sci Res. 2015;23(2):244-52.
[17] Ghosh A, Choi M, Yoon D, Kim S, Kim J, Yee JJ, et al. Stream water quality control and odor reduction through a multistage vortex aerator: a novel in situ remediation technology. Water. 2023;15(11):1982.
[18] Fang L, Xu X, Li A, Wang Z, Li Q. Numerical investigation on the flow characteristics and choking mechanism of cavitation-induced choked flow in a venturi reactor. Chem Eng J. 2021;423:130234.
[19] Lee CH, Choi H, Jerng DW, Kim DE, Wongwises S, Ahn HS. Experimental investigation of microbubble generation in the venturi nozzle. Int J Heat Mass Transfer. 2019;136:1127-38.
[20] Sakamatapan K, Mesgarpour M, Mahian O, Ahn HS, Wongwises S. Experimental investigation of the microbubble generation using a venturi-type bubble generator. Case Stud Therm Eng. 2021;27:101238.
[21] American Society of Civil Engineers. Measurement of oxygen transfer in clean water. Reston: American Society of Civil Engineers; 2007.
[22] Adel M, Shaalan MR, Kamal RM, El Monayeri DS. A comparative study of impeller aerators configurations. Alexandria Eng J. 2019;58(4):1431-8.